



# Nd isotopic composition of water masses and dilution of the Mediterranean outflow along the southwest European margin

## K. Copard

*Laboratoire des Interactions et Dynamique des Environnements de Surface, UMR 8148, CNRS, Université de Paris-Sud, Bâtiment 504, F-91405 Orsay CEDEX, France (copard.kevin@gmail.com)*

*Laboratoire des Sciences du Climat et de l'Environnement, Laboratoire mixte CNRS-CEA, Avenue de la Terrasse, F-91198 Gif-sur-Yvette CEDEX, France*

## C. Colin

*Laboratoire des Interactions et Dynamique des Environnements de Surface, UMR 8148, CNRS, Université de Paris-Sud, Bâtiment 504, F-91405 Orsay CEDEX, France*

## N. Frank

*Laboratoire des Sciences du Climat et de l'Environnement, Laboratoire mixte CNRS-CEA, Avenue de la Terrasse, F-91198 Gif-sur-Yvette CEDEX, France*

## C. Jeandel

*Laboratoire d'Etudes en Géophysique et Océanographie Spatiale, UMR 5566, CNRS, Observatoire Midi-Pyrénées, 14 Avenue E. Belin, F-31400 Toulouse, France*

## J.-C. Montero-Serrano

*Laboratoire des Interactions et Dynamique des Environnements de Surface, UMR 8148, CNRS, Université de Paris-Sud, Bâtiment 504, F-91405 Orsay CEDEX, France*

*Laboratoire des Sciences du Climat et de l'Environnement, Laboratoire mixte CNRS-CEA, Avenue de la Terrasse, F-91198 Gif-sur-Yvette CEDEX, France*

## G. Reverdin

*Laboratoire d'Océanographie et de Climatologie par Expérimentation et Analyse Numérique, Institut Pierre Simon Laplace, Université Pierre et Marie Curie, Case 100, 4 Place Jussieu, F-75252 Paris CEDEX 05, France*

## B. Ferron

*Laboratoire de Physique des Océans, UMR 6523, IFREMER, Centre de Brest, F-29280 Plouzané, France*

[1] Nd isotopic compositions ( $\epsilon\text{Nd}$ ) of seawater profiles and deep-sea corals collected off the coast of Iberia and from the Bay of Biscay were measured (1) to constrain the Nd isotopic composition of water masses along the southwest European margin, (2) to track the Mediterranean Outflow Water (MOW) during its northward propagation, and (3) to establish hydrological changes during the last 1500 years. The Eastern North Atlantic Central Water (ENACW) is characterized by Nd isotopic composition of around  $-12.0$ . Mediterranean Sea Water (MSW) is collected from 800 and 1200 m depth and is characterized by  $\epsilon\text{Nd}$  values ranging from  $-10.9$ , off the coast of Iberia, to  $-11.6$  in the Bay of Biscay. These  $\epsilon\text{Nd}$  results suggest a strong dilution of the pure MOW at the Strait of Gibraltar ( $\epsilon\text{Nd} -9.4$ ) of approximately 40%

and 30% along its northward circulation pathway essentially with a contribution from ENACW. At around 2000 m depth,  $\epsilon\text{Nd}$  water profiles display the occurrence of a nonradiogenic water mass ( $\epsilon\text{Nd} -13$ ), originating from the Labrador Sea (Labrador Sea Water). Fossil deep-sea corals, dated between 84 and 1500 years, display Nd isotopic compositions that vary moderately from present-day seawater values, suggesting a weaker influence of MOW in the formation of MSW during the Dark Ages and the Little Ice Age. These recent cold events seem to be associated with a reduction in the northward penetration of MSW, which may result from a greater eastward extension of the middepth subpolar gyre and/or a reduction of MSW formation, likely tied to a variation in deep Mediterranean water production.

**Components:** 9100 words, 6 figures, 3 tables.

**Keywords:** European margin; Nd isotopic composition; deep-sea corals; water masses.

**Index Terms:** 0454 Biogeosciences: Isotopic composition and chemistry (1041, 4870).

**Received** 25 January 2011; **Revised** 7 April 2011; **Accepted** 9 April 2011; **Published** 30 June 2011.

Copard, K., C. Colin, N. Frank, C. Jeandel, J.-C. Montero-Serrano, G. Reverdin, and B. Ferron (2011), Nd isotopic composition of water masses and dilution of the Mediterranean outflow along the southwest European margin, *Geochem. Geophys. Geosyst.*, 12, Q06020, doi:10.1029/2011GC003529.

## 1. Introduction

[2] In the ocean, dissolved Nd is a trace element of lithogenic origin characterized by a residence time of approximately 500 to 1000 years [Tachikawa *et al.*, 2003]. The Nd isotopic composition corresponds to the  $^{143}\text{Nd}/^{144}\text{Nd}$  ratio and is expressed as  $\epsilon\text{Nd}$ .  $\epsilon\text{Nd}$  is defined by  $\epsilon\text{Nd} = ((^{143}\text{Nd}/^{144}\text{Nd})_{\text{sample}} / (^{143}\text{Nd}/^{144}\text{Nd})_{\text{CHUR}} - 1) * 10000$ , where CHUR stands for Chondritic Uniform Reservoir and represents a present-day average earth value:  $(^{143}\text{Nd}/^{144}\text{Nd})_{\text{CHUR}} = 0.512638$  [Jacobsen and Wasserburg, 1980]. The Nd isotopic composition of the continents is heterogeneous. It was shown that through the Nd isotopic composition gradients of continental margins, water masses acquire a characteristic Nd isotopic signature that is subsequently modified by the mixing of these water masses or by geochemical processes at the continental margin, referred to as boundary exchange [Lacan and Jeandel, 2005a]. This observation encouraged the study of the Nd isotopic composition of seawater to trace the origin of water masses in modern oceanography [e.g., Lacan and Jeandel, 2004a, 2005b; Piepgras and Wasserburg, 1983; Spivack and Wasserburg, 1988; Tachikawa *et al.*, 2004] and to trace the provenance and advection strength of water masses in the past [Burton and Vance, 2000; Vance and Burton, 1999; Piotrowski *et al.*, 2004, 2005; Colin *et al.*, 2010].

[3] Numerous studies have been conducted to identify the water mass signatures and temporal evolution of Nd isotopic gradients in the North Atlantic

[Piepgras and Wasserburg, 1983, 1987; Spivack and Wasserburg, 1988; Lacan and Jeandel, 2005b]. The North Atlantic is a region of complex hydrological patterns driven by surface gyre circulations, the northward advection of water from the temperate Atlantic, intermediate water recirculation, and the formation and southward propagation of North Atlantic Deep Water (NADW). Although many of the water masses of the complex Atlantic circulation patterns have already been investigated on both modern and millennial times scales using deep-sea sediments and corals [van de Flierdt *et al.*, 2006; Colin *et al.*, 2010; Copard *et al.*, 2010], little is known about the Nd isotopic composition of modern seawater from the Eastern margin of the North Atlantic. However, this information is crucial to establishing the Nd isotopic composition of water masses such as the Eastern North Atlantic Central Water (ENACW) and the Mediterranean Sea Water (MSW). These water masses flow along the European margin and penetrate into the Rockall Trough [Lozier and Stewart, 2008] where they can mix and influence other water masses flowing northward before they enter into Nordic Seas and are downwelled. Here, we present  $\epsilon\text{Nd}$  measurements of two water profiles along the Western European margin (Bay of Biscay and off the Iberian Peninsula) to better characterize water masses circulation in this region and to track the northward transport and evolution of the Nd isotopic composition of MSW and ENACW. The Nd isotopic composition of these water masses is then compared to the Nd isotopic composition of both modern and fossil deep-sea corals (*L. Pertusa*, *M. oculata*, *D. dianthus*) collected

at variable depths in the Bay of Biscay and off the Iberian Peninsula. The Nd isotopic composition of deep-sea corals is then used to determine the potential variability of the  $\epsilon\text{Nd}$  of the Western European water masses through time and thus to track hydrological changes along the Eastern margin of the North Atlantic during the last 1500 years.

## 2. Hydrological Setting

[4] Along the Western European margin, a subsurface water mass, called the Eastern North Atlantic Central Water (ENACW), is formed by the subduction of water during winter. The ENACW is located between the seasonal thermocline and the lower part of the permanent thermocline. In the Gulf of Cadiz, this water mass occurs between 100 and 600 m [Louarn, 2008].

[5] At the Strait of Gibraltar, two layers of water can be distinguished by a sharp density gradient: the eastward flow of low-density Atlantic water (ENACW) overlies the more saline westward outflow of high-density Mediterranean water corresponding to the MOW. The MOW is characterized by high salinities ( $S > 36.9\text{‰}$ ), temperatures ranging from 13.22 to 13.76°C, a density  $>28.8\text{ kg m}^{-3}$  and an  $\epsilon\text{Nd}$  value of  $-9.4$  [Tachikawa *et al.*, 2004; Spivack and Wasserburg, 1988]. At the exit of the Gulf of Cadiz, the MOW is strongly modified by vertical mixing with the overlying ENACW during its overflow and is thus referred to as Mediterranean Sea Water (MSW). In the Gulf of Cadiz, two layers of the MSW have been discriminated. The upper layer of the MSW ( $\text{MSW}_u$ ) lies between 800 and 900 m and the lower layer of the MSW ( $\text{MSW}_l$ ) occurs at depths of 1100–1200 m.

[6] The presence of Antarctic Intermediate Water (AAIW) has also been identified in the  $\text{MSW}_l$  in the Gulf of Cadiz [Louarn, 2008]. However, AAIW is present only in the southern part of the Gulf of Cadiz and comprises a small proportion ( $<10\%$ ) of the total water mass and does not flow further North along the European coast [Louarn, 2008]. The upper layer of MSW is then composed of MOW and ENACW and its lower layer is composed of MOW, ENACW and AAIW [Louarn, 2008]. The Nd isotopic composition of MSW is not well determined and depends on the rate of mixing between MOW ( $\epsilon\text{Nd} = -9.4$ ) and the surrounding water masses (mainly the ENACW) during the overflow.

[7] Below intermediate waters ( $\text{MSW}$  and AAIW), the study area is characterized at 2000 m depth by

the presence of the Labrador Sea Water (LSW) [van Aken, 2000; Forner, 2005; Ait-Ameur and Goyet, 2006; Louarn, 2008]. At even greater depths, Lower Deep Water (LDW) flows north [van Aken, 2000]. This deep water mass results from the mixing of Antarctic Bottom Water (AABW) and the less dense Eastern North Atlantic Deep Water (ENADW) as it flows northward through the Atlantic Ocean.

## 3. Material and Methods

[8] Ten seawater samples were collected during the OVIDE cruise off the Iberian Peninsula (Ovide station 15: 40°20'N; 12°13.21'W) in June 2008. Eleven seawater samples were collected during the CAROLS cruise in the Bay of Biscay, in November 2008 (Figure 1 and Table 1). Samples were collected at both sites in the upper 3000 m of the water column.

[9] Eighteen deep-sea corals (*L. Pertusa*, *M. oculata*, *D. dianthus*) from the collection of the MNHN (Muséum national d'Histoire naturelle de Paris) were originally collected off the Iberian Peninsula and along the slope of the Bay of Biscay during BIOGAS I cruise and several THALASSA cruises (1972–1973) (Figure 1 and Table 2). Two additional deep-sea coral samples (B08–04) were collected during the BISCOT cruise in 2008 (Figure 1 and Table 2).

[10] Nd isotopic compositions of seawater were analyzed on unfiltered samples following the analytical procedures described by Lacan and Jeandel [2001]. Briefly, the Nd was extracted from approximately 15 L of seawater by ion exchange chromatography. Seawater rare earth elements (REE) were preconcentrated using SEP-PAK Classic C18 cartridges loaded with a HDEHP.H<sub>2</sub>.MEHP complexant. REE were then purified using a cationic resin (AG50X8). Nd was purified using an Ln-Spec column, following the method described in detail by Copard *et al.* [2010].  $^{143}\text{Nd}/^{144}\text{Nd}$  ratios of seawater samples were performed using static multicollection on a Finnigan MAT-262 at the Laboratoire des Sciences du Climat et de l'Environnement (LSCE, CEA-CNRS-UVSQ, Gif/Yvette).  $^{143}\text{Nd}/^{144}\text{Nd}$  ratios were corrected for mass fractionation relative to  $^{146}\text{Nd}/^{144}\text{Nd} = 0.7219$  using a power law. Blank values were  $<500\text{ pg}$ . These values can be neglected as they represent less than 1.5% of the total seawater samples (taking account the volume of the seawater sample (15 L) and the Nd concentration of seawater in the study area). Replicate analyses ( $n = 30$ ) of the La Jolla standard gave a mean  $^{143}\text{Nd}/^{144}\text{Nd}$

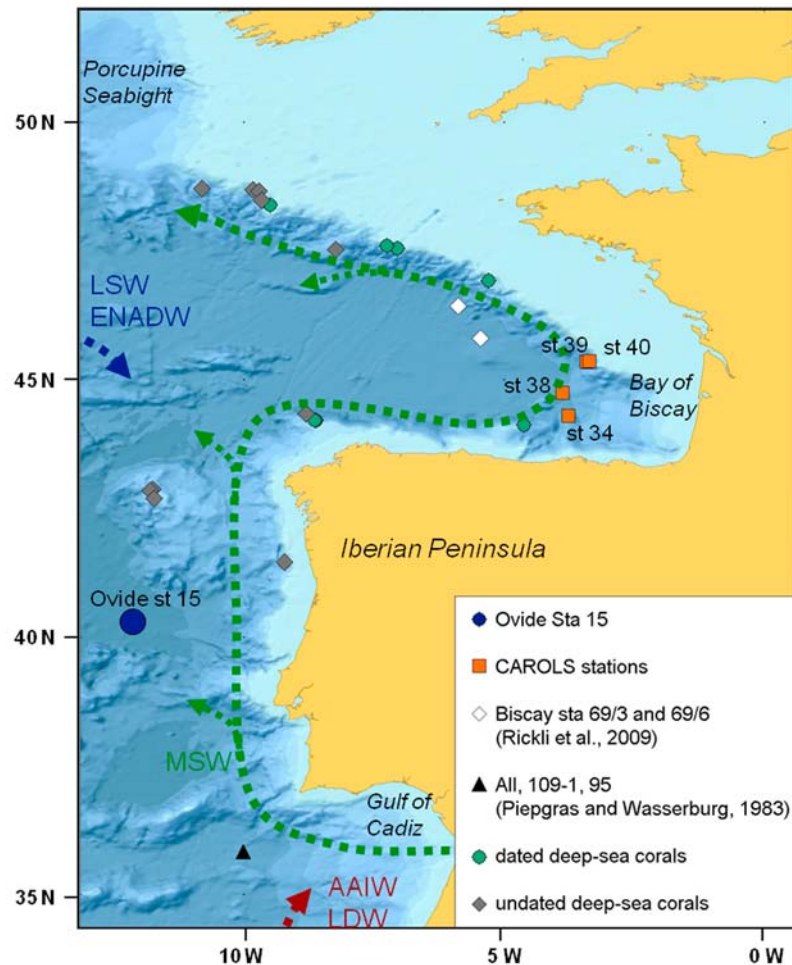


**Figure 1.** Location of Ovide station 15 (blue circle), CAROLS stations (gold squares), and deep-sea corals (green circles, gray diamonds) investigated in this study. Undated corals are represented by gray diamonds, dated corals are represented by green circles. Seawater stations 69/3 and 69/6 (white diamonds) investigated by *Rickli et al.* [2009] and station 95 of cruise 109–1 RV Atlantis II (black triangle) investigated by *Piepgras and Wasserburg* [1983] are also reported. Water masses circulating in this region are Mediterranean Sea Water (MSW), Eastern North Atlantic Central Water (ENACW), Antarctic Intermediate Water (AAIW), Antarctic Bottom Water (AABW), Labrador Sea Water (LSW) and Eastern North Atlantic Deep Water (ENADW).

La Jolla =  $0.511859 \pm 0.000014$  which is within the uncertainty of its certified value of  $0.511850 \pm 0.000013$ .

[11] Deep-sea corals are often exposed to seawater for a long time and may acquire a black coating of ferromanganese oxides and hydroxides. Rigorous cleaning techniques were therefore applied, following the procedure presented by *Copard et al.* [2010], to avoid contamination of Nd isotopic composition by these coatings. This procedure consists mainly of carefully polishing the inner and outermost surface of the coral skeletons using a diamond blade saw to retrieve an opaque and translucent pure aragonite skeleton. This mechanical cleaning was followed by two weak attacks with dilute ultraclean 0.5 N

hydrochloric acid in an ultrasonic bath for 10 min to remove further potential residual Fe-Mn coatings. A Nd-oxide technique for thermal ionization mass spectrometry (TIMS) was used to determine the Nd isotopic composition ( $^{143}\text{Nd}/^{144}\text{Nd}$  ratios) of deep-sea corals. The chemical purification of Nd, using TRU-Spec resin and Ln-Spec resin as well as the mass spectrometric techniques applied here are described in detail by *Copard et al.* [2010]. Nd cuts were loaded onto a single Re degassed filaments and run using the  $\text{H}_3\text{PO}_4/\text{silica}$  gel method. Samples were analyzed for two hundred  $^{143}\text{Nd}/^{144}\text{Nd}$  ratios with a monitor beam ( $^{144}\text{Nd}^{16}\text{O}$ ) higher than 500 mV on a six Faraday collector Finnigan MAT 262 TIMS (LSCE, Gif/Yvette).  $\text{PrO}^+$  isobaric interferences were measured and corrected line by line during

**Table 1.** Locations of Seawater Stations Investigated in This Study With Water Depth of Sampling<sup>a</sup>

Station	Location Latitude	Longitude	Depth (m)	$\theta$ (°C)	S (psu)	$\sigma\theta$ (kg m <sup>-3</sup> )	$\epsilon\text{Nd}$ ( $\pm 0.3$ )
OVIDE st 15	40°20'N	12°13.21'W	97	14.00	35.95	26.92	-11.3
	40°20'N	12°13.21'W	296	12.06	35.68	27.11	-11.8
	40°20'N	12°13.21'W	396	11.50	35.61	27.16	-12.0
	40°20'N	12°13.21'W	496	11.33	35.64	27.21	-12.0
	40°20'N	12°13.21'W	751	10.71	35.78	27.44	-11.4
	40°20'N	12°13.21'W	904	10.37	35.88	27.58	-11.1
	40°20'N	12°13.21'W	1200	10.29	36.08	27.74	-10.9
	40°20'N	12°13.21'W	1504	7.15	35.53	27.82	-11.7
	40°20'N	12°13.21'W	2010	3.98	35.04	27.82	-13.0
40°20'N	12°13.21'W	2988	2.82	34.95	27.86	-12.2	
CAROLS st 40	45°21.2'N	3°22.5'W	140	12.18	35.65	27.02	-10.7
CAROLS st 38	44°44.1'N	3°54.0'W	198	12.18	35.66	27.06	-11.0
CAROLS st 34	44°17.4'N	3°46.9'W	302	11.75	35.63	27.07	-11.7
CAROLS st 34	44°17.4'N	3°46.9'W	402	11.49	35.60	27.13	-11.6
CAROLS st 38	44°44.1'N	3°54.0'W	547	11.08	35.61	27.17	-11.5
CAROLS st 38	44°44.1'N	3°54.0'W	799	10.44	35.72	27.25	-11.2
CAROLS st 38	44°44.1'N	3°54.0'W	1110	9.36	35.77	27.45	-11.5
CAROLS st 38	44°44.1'N	3°54.0'W	1500	6.27	35.33	27.69	-12.2
CAROLS st 38	44°44.1'N	3°54.0'W	1825	4.61	35.11	28.00	-12.7
CAROLS st 39	45°20.1'N	3°26.7'W	2135	3.66	35.02	27.83	-11.8
CAROLS st 39	45°20.1'N	3°26.7'W	2635	2.97	34.96	27.85	-11.4

<sup>a</sup>Potential temperature ( $\theta$ ), salinity (S), and potential density ( $\sigma\theta$ ) and  $\epsilon\text{Nd}$  data results are reported.  $\epsilon\text{Nd}$  are given with a reproducibility of  $\pm 0.3$  ( $2\sigma$ ).

offline analysis. The Nd isotopic ratios were corrected for mass fractionation relative to  $^{146}\text{Nd}/^{144}\text{Nd} = 0.7219$  using a power law. Oxygen isotope ratios used for the corrections are  $^{18}\text{O}/^{16}\text{O} = 0.002085$  and  $^{17}\text{O}/^{16}\text{O} = 0.000391$ . Concentrations of Nd in the blanks were negligible compared to the concentrations of Nd in the deep-sea corals investigated in this study. Replicate analyses ( $n = 124$ ) of the La Jolla standard gave a mean  $^{143}\text{Nd}/^{144}\text{Nd}$  of  $0.511858 \pm 0.000010$ . This mean value is close to the certified value of  $0.511850 \pm 0.000013$ , suggesting a negligible (0.00001) machine bias that was taken into consideration for the sample data's re-treatment following a bracketing technique.

[12] Ca, Mn and Nd concentrations of deep-sea corals were determined on same cleaned samples than those used for Nd isotopic composition determinations in order to evaluate the efficiency of the cleaning procedure and to discard any deep-sea corals samples presenting residual ferromanganese coatings. These analyses were conducted at the LSCE using a quadruple ICP-MS Xseries II CCT (Thermo Fisher Scientific) to measure the isotopes  $^{46}\text{Ca}$ ,  $^{55}\text{Mn}$  and  $^{146}\text{Nd}$  [Copard *et al.*, 2010].

[13] Six deep-sea corals investigated in this study have been dated by  $^{230}\text{Th}/\text{U}$  method (Table 2). U-isotopic measurements were carried out using an ICPQMS (ThermoX-series - Gif-sur-Yvette) according to the procedures of Douville *et al.* [2010]. Th isotopic measurements were carried out using a MC-

ICPMS to obtain higher precision (ThermoFisher Neptune - IPG Paris). Reproducibility and accuracy of analyses were determined through frequent measurements of HU1 standard solution spiked with an in-house  $^{229}\text{Th}$ ,  $^{233}\text{U}$ ,  $^{236}\text{U}$  triple spike and yield <5‰ reproducibility for U isotope measurements and <8‰ for Th isotope measurements.

## 4. Results

### 4.1. Hydrological Parameters

[14] Potential temperature, salinity and potential density results from the 21 seawater samples are reported in Table 1. The salinity versus potential temperature and salinity versus water depth diagrams (Figures 2a and 2b) allow the identification of similar water masses at both stations: ENACW, MSW as well as deeper and fresher water masses (LSW, LDW). At Ovide station 15, potential temperatures range from 14.0°C to 2.82°C and salinities from 36.08‰ to 34.95‰. For the CAROLS stations, potential temperatures are between 12.18°C and 2.97°C and the salinity varies between 35.77‰ and 34.96‰. The core of ENACW is identifiable at approximately 400 m depth, at both station, by a salinity minimum of 35.6‰ and a temperature of 11.5°C. At approximately 1100–1200 m depth, the core of MSW is characterized by a salinity maximum of 36.1‰ and a temperature of 10.3°C off the Iberian Peninsula and a salinity maximum of 35.8‰



**Table 2.** U Series Measurements and Ages of Fossil Corals Investigated in This Study<sup>a</sup>

Labcode	Sample	<sup>238</sup> U (ppm)	<sup>232</sup> Th (ppb)	$\delta^{234}\text{U}_M$ (‰)	$(^{230}\text{Th}/^{238}\text{U})$	$(^{230}\text{Th}/^{232}\text{Th})$	Age (kyr)	$\delta^{234}\text{U}_T$ (‰)	Age* (kyr)
Gif-1455	MNHN Gasc L535	3.838 ± 0.004	0.161 ± 0.007	146.4 ± 1.9	0.0010 ± 0.0001	73.5 ± 6.7	97 ± 8	146.4 ± 1.9	84 ± 8
Gif-1456	MNHN Gasc L600	4.131 ± 0.004	0.641 ± 0.044	145.4 ± 1.7	0.0019 ± 0.0002	37.3 ± 4.6	181 ± 19	145.5 ± 1.7	133 ± 19
Gif-1462	MNHN Gasc L900	2.821 ± 0.003	0.496 ± 0.016	145.0 ± 2.4	0.0029 ± 0.0003	51.0 ± 5.8	281 ± 32	145.2 ± 2.4	226 ± 32
Gif-1463	MNHN Gasc L950	3.165 ± 0.004	0.478 ± 0.021	147.6 ± 2.8	0.0021 ± 0.0003	42.7 ± 5.9	202 ± 27	147.7 ± 2.8	155 ± 27
Gif-1466	MNHN Gasc D600	4.119 ± 0.004	2.058 ± 0.113	144.9 ± 2.0	0.0069 ± 0.0003	42.4 ± 3.0	664 ± 32	145.2 ± 2.0	508 ± 32
Gif-1467	MNHN Gasc D825	3.161 ± 0.006	0.283 ± 0.014	143.9 ± 1.1	0.0160 ± 0.0004	544.4 ± 29.0	1534 ± 37	144.5 ± 1.1	1506 ± 37

<sup>a</sup>Age\* reflects ages calculated based on a simple correction model considering precipitation of initial <sup>230</sup>Th from seawater taking seawater (<sup>232</sup>Th/<sup>230</sup>Th) activity ratios ranging from 14 to 6 into account [Frank et al., 2004].

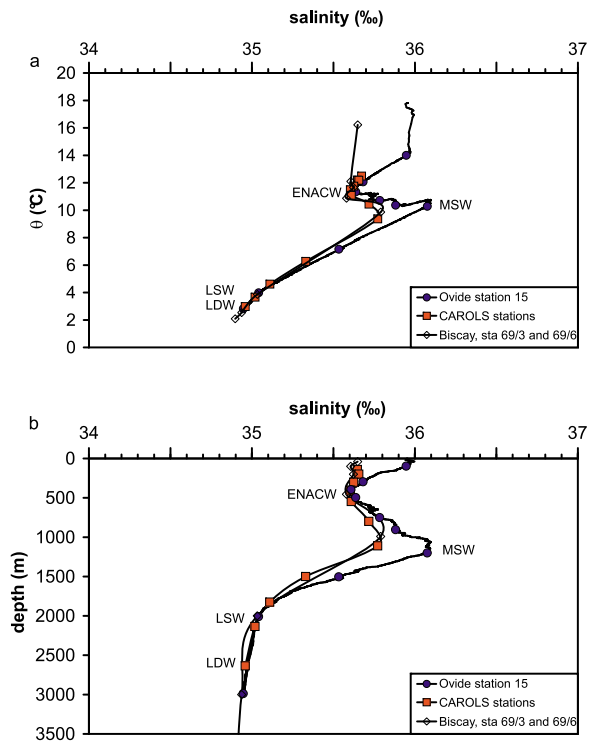


**Figure 2.** (a) Potential temperature (°C) versus salinity (PSU) for Ovide station 15 (blue circles) and CAROLS stations 69/3 and 69/6 (open diamonds) compared to Biscay stations 69/3 and 69/6 (open diamonds) obtained by Rickli et al. [2009] and (b) salinity (PSU) versus water depth (m) obtained for Ovide station 15 (blue circles) and CAROLS stations (gold squares), compared to Biscay stations 69/3 and 69/6 (open diamonds) obtained by Rickli et al. [2009].

and a temperature of 9.4°C in the Bay of Biscay. The deepest water masses are characterized by a minimum of salinity and temperature of 34.95‰ and 2.8°C at Ovide station 15 and of 34.96‰ and 2.97°C at the CAROLS stations.

## 4.2. Seawater εNd Results

[15] The Nd isotopic compositions of seawater samples analyzed are reported in Table 1. εNd values for Ovide station 15 and the CAROLS stations seawater samples range from  $-13.0 ± 0.3$  to  $-10.9 ± 0.3$  and from  $-12.7 ± 0.3$  to  $-10.7 ± 0.3$ , respectively. The Nd isotopic compositions exhibit large variations at both stations along the entire depth profile (Figure 3).

[16] For OVIDE station 15 seawater (Figure 3a), εNd reaches its first minimum between 396 and 496 m depth, with values around  $-12.0 ± 0.3$ , and the second minimum occurs at 2010 m depth, with a value of  $-13.0 ± 0.3$  whereas an εNd maximum of  $-10.9 ± 0.3$  occurs at 1200 m depth. For the

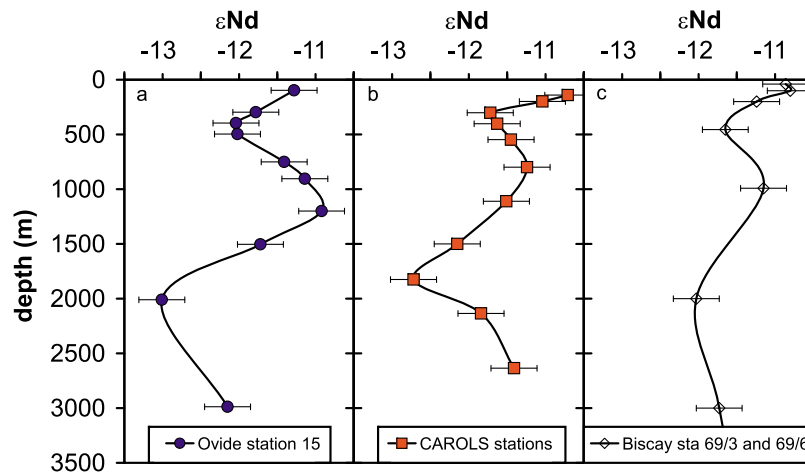


**Figure 3.** Seawater  $\epsilon\text{Nd}$  versus water depth (m) obtained for (a) Ovide station 15 (blue circles), (b) CAROLS stations (gold squares) and (c) compared to Biscay stations 69/3 and 69/6 (open diamonds) measured by Rickli *et al.* [2009].

CAROLS stations (Figure 3b),  $\epsilon\text{Nd}$  follows the same pattern but with less pronounced variations. Two  $\epsilon\text{Nd}$  minima occur, the first around 300 m depth, with a value of  $-11.7 \pm 0.3$ , and the second around 1800 m depth, with a value of  $-12.7 \pm 0.3$ . An  $\epsilon\text{Nd}$  maximum of  $-11.2 \pm 0.3$  occurs at approximately 800 m depth.

### 4.3. Age and $\epsilon\text{Nd}$ of Deep-Sea Corals

[17] Ages of the six deep-sea corals obtained by  $^{230}\text{Th}/\text{U}$  dating are reported in the Table 2. U concentrations range from  $2.821 \pm 0.003$  and  $4.131 \pm 0.004$  ppm. These values are similar to the values obtained from other cold-water corals analyzed by Frank *et al.* [2004] and Copard *et al.* [2010]. Th/U ages are given as measured and corrected (\*) ages, based on measured ( $^{230}\text{Th}/^{238}\text{U}$ ) and ( $^{234}\text{U}/^{238}\text{U}$ ) activity ratios [Frank *et al.*, 2004] and using the half-lives of Cheng *et al.* [2000]. Corrected ages include a correction for  $^{230}\text{Th}$  derived from seawater, which is based on an estimated seawater ( $^{230}\text{Th}/^{232}\text{Th}$ ) activity ratio ranging from 5 to 12 (Station L3 [Vogler *et al.*, 1998]). The corrected age of the six deep-sea corals investigated in this study ranges from  $84 \pm 8$  to  $1506 \pm 37$  years (Table 2). In addition, the two corals samples B08-04-E2 and B08-04-E3, taken during the BISCOT cruise, were collected from a coral polyp that was living when it was sampled. Thus, we can assume that these two deep-sea corals are approximately less than 30 years.

[18] Nd concentrations, Nd/Ca and Mn/Ca ratios, and  $\epsilon\text{Nd}$  of deep-sea corals collected in the Bay of Biscay and off the Galicia Bank are reported in

Table 3 (Figure 1). The Nd concentration of deep-sea corals (*L. pertusa*, *D. Dianthus* and *M. oculata*) ranges from 6.2 to 111.1 ppb and the Mn/Ca ratio is lower than  $4.47 \mu\text{mol}/\text{mol}$  (Table 3). The Mn/Ca ratio is not correlated with the Nd/Ca ratio (correlation coefficient  $r^2 = 0.05$ ) and  $\epsilon\text{Nd}$  (correlation coefficient  $r^2 = 0.09$ ), excluding any significant contamination by Fe-Mn oxy-hydroxides. This range in the Mn/Ca ratio is comparable with ranges observed in several living deep-sea corals by Copard *et al.* [2010], demonstrating that the cleaning procedure used is sufficient to entirely remove the coral coating. Therefore, Nd isotopic compositions analyzed on cleaned coral samples are representative of the Nd incorporated from seawater into the aragonite skeleton.

[19] All deep-sea corals investigated in this study present  $\epsilon\text{Nd}$  values ranging from  $-10.7 \pm 0.4$  to  $-12.3 \pm 0.3$  (Table 3). Undated deep-sea corals (*D. dianthus* and *M. oculata*) from the Galicia Bank (Figure 4a) show  $\epsilon\text{Nd}$  values decreasing from  $-11.3 \pm 0.3$  at a depth of 765 m (Galice M765) and  $-10.9 \pm 0.3$  between 1150 and 1220 m depth (Galice D1150), with an intermediate value of  $-11.2 \pm 0.3$  between 985 and 1000 m depth (Galice M985). These  $\epsilon\text{Nd}$  values are similar to the seawater  $\epsilon\text{Nd}$  profile except for the sample Galice M1110 (undated) collected at 1110 m depth, which presents a lower  $\epsilon\text{Nd}$  value of  $-12.0 \pm 0.3$  (Figure 4a).

[20] In the Bay of Biscay, deep-sea corals of different species (*L. pertusa*, *D. dianthus* and *M. oculata*) sampled between 535 and 800 m depth show similar  $\epsilon\text{Nd}$  values between  $-11.3 \pm 0.6$  and  $-11.6 \pm 0.3$  (Figure 4b). Three of them were dated at

**Table 3.** Location, Species, Age, and Water Depth of the Deep-Sea Coral Samples Investigated in This Study<sup>a</sup>

Sample Name	Species	Latitude	Longitude	Water Depth (m)	Age U-Th (years)	Nd (ppb)	Nd/Ca (nmol/mol)	Mn/Ca ( $\mu$ mol/mol)	$\epsilon$ Nd ( $\pm 2\sigma$ )
MNHN Gasc L535	<i>L. pertusa</i>	44°12.0'N	08°40.7'W	535–548	84 ± 8	11.8	8.33	0.30	-11.4 ± 0.4
MNHN Gasc L600	<i>L. pertusa</i>	44°12.0'N	08°40.8'W	600–625	133 ± 19	110.1	82.30	1.11	-11.5 ± 0.3
MNHN Gasc D600	<i>D. dianthus</i>	44°07.0'N	04°38.8'W	600–655	508 ± 32	92.7	69.35	2.91	-11.6 ± 0.3
B08-04-E2	<i>M. oculata</i>	46°54.4'N	05°19.4'W	693	living	11.8	8.0	0.17	-11.4 ± 0.3
B08-04-E3	<i>M. oculata</i>	46°54.4'N	05°19.4'W	693	living	14.2	9.9	0.19	-10.7 ± 0.4
MNHN Gasc L700	<i>L. pertusa</i>	48°27.9'N	09°44.0'W	700	undated	7.0	5.02	2.58	-11.5 ± 0.6
MNHN Gasc L750	<i>L. pertusa</i>	43°57.3'N	05°44.2'W	700–750	undated	8.1	6.49	0.10	-11.5 ± 0.8
MNHN Gasc L800	<i>L. pertusa</i>	48°38.2'N	09°47.3'W	800	undated	6.2	4.52	0.07	-11.3 ± 0.6
MNHN Gasc D825	<i>D. dianthus</i>	47°34.8'N	07°18.1'W	825	1506 ± 37	30.3	22.49	3.60	-11.7 ± 0.3
MNHN Gasc L900	<i>L. pertusa</i>	47°32.4'N	07°06.8'W	900	226 ± 32	25.3	19.17	0.18	-11.9 ± 0.4
MNHN Gasc L950	<i>L. pertusa</i>	48°22.5'N	09°33.5'W	950	155 ± 27	9.0	6.64	0.08	-11.2 ± 0.3
MNHN Gasc L1050	<i>L. pertusa</i>	48°39.7'N	09°53.2'W	1050	undated	40.0	29.52	0.28	-11.1 ± 0.8
MNHN Gasc D1050	<i>D. dianthus</i>	48°39.7'N	09°53.2'W	1050	undated	53.9	40.39	0.63	-11.6 ± 0.3
MNHN Gasc D1420	<i>D. dianthus</i>	48°41.5'N	10°53.0'W	1420–1470	undated	111.1	83.98	0.38	-12.2 ± 0.2
MNHN Gasc L2090	<i>L. pertusa</i>	47°30.6'N	08°17.5'W	2090	undated	15.7	11.68	0.90	-11.7 ± 0.4
MNHN Gasc D2400	<i>D. dianthus</i>	44°20'N	08°52'W	2400–2700	undated	98.5	74.69	1.48	-12.3 ± 0.3
MNHN Galice M765	<i>M. oculata</i>	42°41.6'N	11°48.5'W	765	undated	11.7	9.06	4.47	-11.3 ± 0.3
MNHN Galice M985	<i>M. oculata</i>	42°52.4'N	11°50.6'W	985–1000	undated	12.8	9.75	3.93	-11.2 ± 0.3
MNHN Galice M1110	<i>M. oculata</i>	42°50.9'N	11°53.1'W	1110–1125	undated	12.0	9.45	0.10	-12.0 ± 0.3
MNHN Galice D1150	<i>D. dianthus</i>	41°28.0'N	09°16.7'W	1150–1220	undated	73.8	57.58	1.43	-10.9 ± 0.3

<sup>a</sup>Results of Nd concentration, Nd/Ca ratio, Mn/Ca ratio, and  $\epsilon$ Nd value are also presented.

84 ± 8 years (*L. pertusa* at 535–548 m depth), 133 ± 19 years (*L. pertusa* at 600–625 m depth) and 508 ± 32 years (*D. dianthus* at 600–655 m depth). Between 825 and 900 m depth, two deep-sea corals dated at 1506 ± 37 (*D. dianthus* at 825 m depth) and 226 ± 32 years (*L. pertusa* at 900 m depth) present  $\epsilon$ Nd values of -11.7 ± 0.3 and -11.9 ± 0.4, respectively. These values are slightly lower than the actual  $\epsilon$ Nd value of seawater (Figure 4).

[21] At greater water depths, the  $\epsilon$ Nd values of two deep-sea corals located at 950 m depth (dated at 155 ± 27 years) and 1050 m depth (undated sample) increase to -11.1, before decreasing to -12.2 ± 0.2 at 1420–1470 m depth (undated sample) and -11.7 at 2090 m depth (undated sample). The deepest deep-sea coral (undated) analyzed in this study (between 2400 and 2700 m depth) has an  $\epsilon$ Nd value of -12.3, which is lower than modern seawater at the same depth.

## 5. Discussion

### 5.1. Nd Isotopic Composition of Water Masses and Dilution of the MOW

[22] Vertical variations in  $\epsilon$ Nd for both seawater stations observed in this study present similar downward variations to those obtained by *Rickli et al.* [2009] in two seawater stations located in the Bay of Biscay (Biscay, sta 69/3 and sta 69/6) reported in Figure 1. The upper layer of the water

column (around 300 and 500 m depth) is composed of ENACW, which is characterized by an isotopic composition of -11.7 at approximately 300 m depth in the Bay of Biscay and -12.0 at 400–500 m depth off the coast of Portugal.

[23] The MSW is characterized by an  $\epsilon$ Nd maximum that reaches -10.9 ± 0.3 at 1200 m depth near the Iberian Peninsula and -11.2 ± 0.3 at 799 m depth in the Bay of Biscay. These values are almost identical to the  $\epsilon$ Nd value of -11.1 ± 0.3 obtained by *Rickli et al.* [2009] in the Bay of Biscay at stations 69/3 and 69/6 (Figures 1 and 3c). In addition, both vertical profiles of  $\epsilon$ Nd in seawater indicate that this maximum of  $\epsilon$ Nd is at a greater depth along the NW Iberian Peninsula than in the Bay of Biscay. At the exit of the Strait of Gibraltar, the MOW is characterized by an  $\epsilon$ Nd of -9.4 [*Tachikawa et al.*, 2004] and a salinity of 38.5‰ [*Spivack and Wasserburg*, 1988]. These  $\epsilon$ Nd and salinity values obtained for the MSW along the Iberian Peninsula and in the Bay of Biscay suggest a strong dilution of the MOW with water masses having a lower radiogenic Nd isotopic composition.

[24] In Figure 5, salinity (‰) is plotted versus  $\epsilon$ Nd to determine the origin of the water mass mixture in the MSW, as well as in greater water depths, and to assess the evolution of water masses as they flow northward. In Figure 5, we have also reported the Nd isotopic composition of the main water masses that were identified in the Gulf of Cadiz (MOW, ENACW, AAIW, LSW, and LDW).

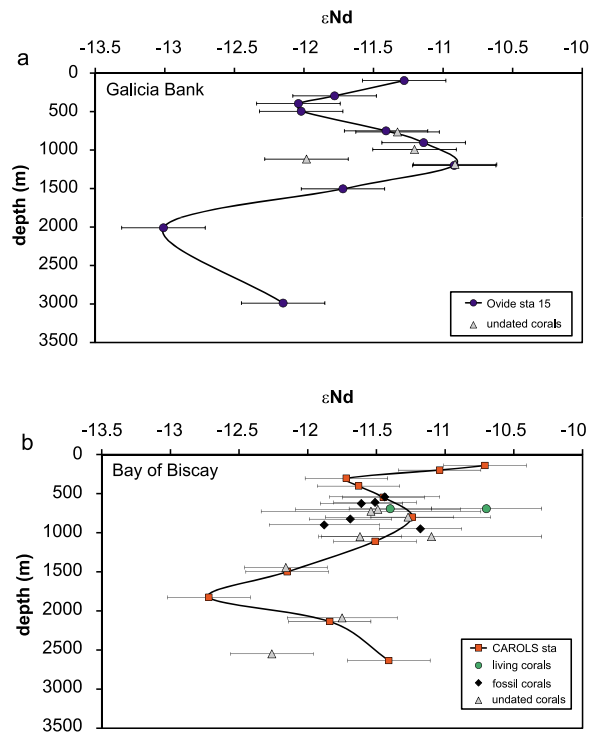


**Figure 4.**  $\epsilon\text{Nd}$  of deep-sea corals versus water depth (m) for (a) the Bank of Galicia and (b) the Bay of Biscay. Undated deep-sea corals are represented by gray triangles, dated corals are represented by black diamonds and living corals are represented by green circles. (c) Seawater  $\epsilon\text{Nd}$  profiles obtained for Ovide station 15 and CAROLS stations are also reported for comparison.

[25] Focusing on the 600–1200 m depth interval (Figure 5a), the water mass evolution off the coast of Iberia and in the Bay of Biscay confirms a mixing between ENACW and MOW. At both stations, we observe that an increase in salinity with depth is associated with increasing  $\epsilon\text{Nd}$  values, reflecting a greater influence of MOW in the mixing balance with depth. In addition, the Southern and Northern stations differ slightly, reflecting the subsequent dilution of MOW along its northward flow path. The  $\epsilon\text{Nd}$  and salinity values do not plot on a straight linear mixing line between the two end-members ENACW and MOW suggesting a moderate nonlinear mixing behavior. This implies the influence of a third water mass. The MSW in the Gulf of Cadiz (station AII 109–1, 101, Figure 1) is influenced by fresher water than MOW but with a quasisimilar Nd isotopic composition. Such characteristics coincide with the occurrence of AAIW in the Gulf of Cadiz, which would influence the mixing described above, as previously suggested by Louarn [2008].

[26] The  $\epsilon\text{Nd}$  value of “pure” ENACW is difficult to assess given the few available studies concerning the Nd isotopic composition of this water mass. Piepgras and Wasserburg [1983] determine an  $\epsilon\text{Nd}$  minimum value of  $-12.5$  at 200 m depth from station 95 of cruise 109–1 RV Atlantis II ( $36^{\circ}17'41''\text{N}$   $10^{\circ}02'27''\text{W}$ ), close to the Gulf of Cadiz (Figure 1). However, it is ambiguous to

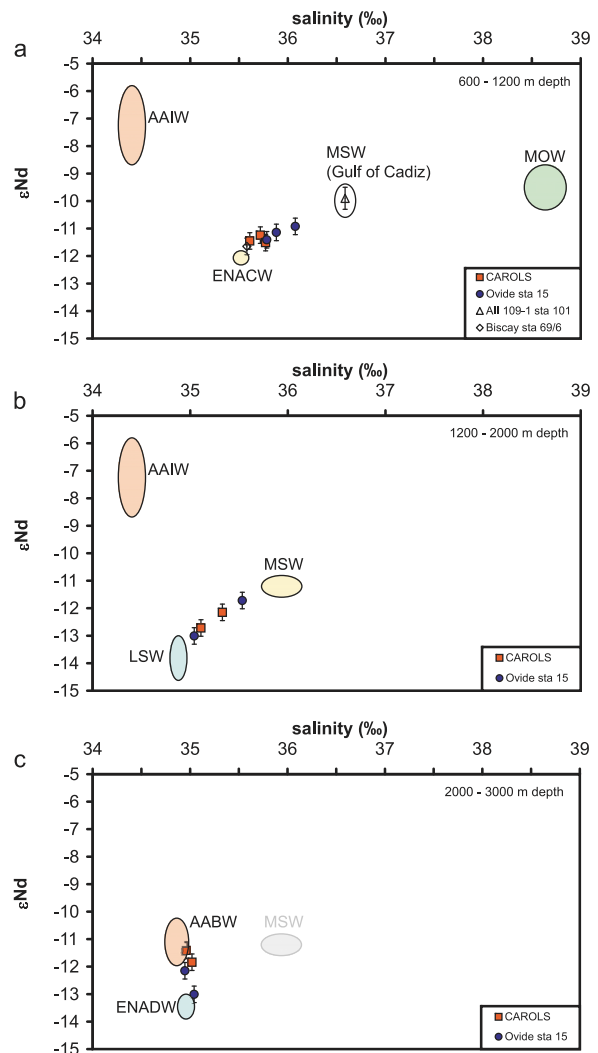


**Figure 5.** Salinity (PSU) versus  $\epsilon\text{Nd}$  obtained for Ovide station 15 (blue circles) and CAROLS stations (gold squares) focused on the (a) 600–1200 m water depth; (b) 1200–2000 m water depth and (c) 2000–3000 m water depth. Potential sources of water masses circulating along the Western European margin are also represented. These water masses include: Mediterranean Outflow Water (MOW), Mediterranean Sea Water (MSW), Eastern North Atlantic Central Water (ENACW), Antarctic Intermediate Water (AAIW), Antarctic Bottom Water (AABW), Labrador Sea Water (LSW) and Eastern North Atlantic Deep Water (ENADW).

affirm that this value corresponds to ENACW as the salinity minimum is observed at 500 m depth for the same station. Here, we obtain an  $\epsilon\text{Nd}$  value of  $-12$  for the ENACW at Ovide station 15. Taking into consideration the  $\epsilon\text{Nd}$  value of MOW at the exit of the Strait of Gibraltar ( $-9.4$  [Tachikawa *et al.*, 2004]), we can estimate that MSW off the coast of Portugal reflects a mixture of approximately 40% of MOW and 60% of ENACW, in agreement with other estimates for the Gulf of Cadiz based on hydrological and tracer data (CFC) [Rhein and Hinrichsen, 1993; Louarn, 2008]. Taking only into account the salinity budgets from both stations and using 35.6‰ for ENACW and 38.5‰ for MOW, we estimate a proportion of approximately 80% of ENACW and 20% of MOW strongly different from previous studies [Rhein and Hinrichsen, 1993; Louarn, 2008] as well as our Nd mixing balance. This is most likely due to the presence of a third low salinity water mass that would lead to an overestimate of ENACW by considering only two end-members.

[27] In the Bay of Biscay, MSW has an  $\epsilon\text{Nd}$  value of  $-11.2 \pm 0.3$ , suggesting a proportion of 30% of MOW in the MSW using the same  $\epsilon\text{Nd}$  values of  $-12$  for ENACW and  $-9.4$  for MOW. However, considering that ENACW is also diluted along its northward circulation, we can suppose that the  $\epsilon\text{Nd}$  value of  $-12$  is underestimated ( $\epsilon\text{Nd} = -11.7$  in the Bay of Biscay) and thus that the proportion of ENACW in MSW is also underestimated and is probably more than 70%. Such estimations are in agreement with a strong dilution of MOW by the surrounding water masses (ENACW) when it flows along the western European margin. This implies that Mediterranean water has a very small influence further North of the Bay of Biscay, such as on the Porcupine Bank and in the Rockall Trough where it is confronted to subpolar gyre or Modified North Atlantic Water entering into the Nordic Seas.

[28] In Figure 5b, for seawater samples collected between 1200 and 2000 m, water masses are getting fresher and unradiogenic, with  $\epsilon\text{Nd}$  value of  $-13.0$  at 2000 m depth off the coast of Portugal and  $-12.7$  at 1800 m depth in the Bay of Biscay. Such Nd isotopic compositions obtained for deep water along the Western European margin indicate the presence of water with a more unradiogenic Nd isotopic composition at around 1800 and 2000 m depth, not highlighted by salinity or temperature profiles (Figure 2). This decrease in  $\epsilon\text{Nd}$  values is also observed by Rickli *et al.* [2009], but with a lower amplitude than in the CAROLS profile probably due to the lower vertical resolution of their analyses (Figure 3). This low  $\epsilon\text{Nd}$  value is

explained by the influence of LSW (Figure 5b), which has an  $\epsilon\text{Nd}$  value of around  $-15$  in the Labrador Sea [Lacan and Jeandel, 2004b].

[29] Below 2000 m (Figure 5c), water masses get more radiogenic, suggesting a mixing between ENADW, coming from the West Atlantic and situated below LSW, and a water mass with higher  $\epsilon\text{Nd}$  values. Spivack and Wasserburg [1988] suggest that the deepest water along the north-west African margin has a southern origin based on its Si concentration. This water, called Lower Deep Water (LDW), is derived from Antarctic Bottom Water AABW (van Aken, 2000) and has also been identified by Forner [2005] along the coast of Western Portugal below 4000 m depth. Between 2000 and 4000 m depth, the LDW mixes mainly with polar waters [Forner, 2005]. The Nd isotopic composition of AABW ranges from  $-10.6$  to  $-11.7$  [Jeandel, 1993] and corresponds to the evolution of  $\epsilon\text{Nd}$  value of the deepest water masses along the West European margin. However, deep water between 2000 and 3000 m in the Bay of Biscay appears to be more radiogenic than off the Iberian Peninsula although the same water masses seem to be present. It is not probable that a higher proportion of LDW is in the Bay of Biscay than off the coast of Portugal as this water originates further south and thus flows along the Portugal margin before entering the Bay of Biscay. Boundary exchange could explain this bias between the two studied areas. Indeed, CARLOS station 39 where the deepest water mass (2635 m) was sampled in the Bay of Biscay is very close to the margin compared to the other study sites. Parra *et al.* [1998, 1999] have determined a mean  $\epsilon\text{Nd}$  value of around  $-10$  for sediments along the margin of the Bay of Biscay which is more radiogenic than deep water in the Bay of Biscay. Consequently, for this deepest water mass boundary exchanges could induce a slight modification of the Nd isotopic composition.

## 5.2. Significance of the $\epsilon\text{Nd}$ of Deep-Sea Corals

[30] For all deep-sea corals that were analyzed in this study, Mn/Ca and Nd/Ca ratios are sufficiently low, implying that Nd isotopic compositions represent those of the deep-sea coral skeletal aragonite [Copard *et al.*, 2010]. In general, the Nd isotopic compositions of modern deep-sea corals (*L. pertusa*, *D. dianthus* and *M. oculata*) investigated in this present study are similar to the Nd isotopic composition for seawater (Figure 4b), confirming the results

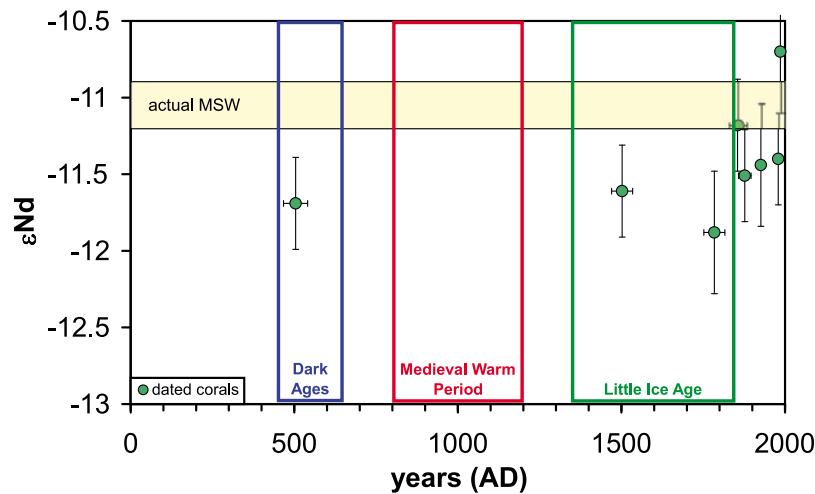


**Figure 6.** Variations in  $\epsilon\text{Nd}$  versus time (years AD) for deep-sea corals, located between 535 and 950 m depth, investigated in this study. The yellow horizontal band corresponds to the actual Nd isotopic composition range of the MSW in the Bay of Biscay and off the coast of Iberia.

of previous studies [Copard *et al.*, 2010; van de Flierdt *et al.*, 2010] that demonstrated that deep-sea corals reliably record the Nd isotopic composition of ambient seawater. Several fossil and undated deep-sea corals display a Nd isotopic composition that differs from seawater suggesting a modification of the  $\epsilon\text{Nd}$  seawater through time (Figure 4).

[31] In Figure 6,  $\epsilon\text{Nd}$  values of dated deep-sea corals are plotted against time for the Bay of Biscay. Three corals located at the depth of the MSW present  $\epsilon\text{Nd}$  values that differ from modern day seawater (Figure 6). These corals are dated at  $1506 \pm 37$  (504 AD),  $508 \pm 32$  (1502 AD) and  $226 \pm 32$  (1784 AD) years. 504 AD corresponds to the Dark Ages Period (450–650 AD [Keigwin and Pickart, 1999; Mikkelsen and Kuijpers, 2001]). Ages of 1502 AD and 1784 AD corresponds to the Little Ice Age (LIA) [Kuijpers *et al.*, 2009; deMenocal *et al.*, 2000; Cronin *et al.*, 2003; Mann *et al.*, 2009]. The Dark Ages Period and the LIA are characterized by colder atmospheric temperatures over Europe and by colder sea surface temperatures over the high latitude of the North Atlantic than today.

[32] The first hypothesis that could be proposed to explain the observed variation in fossil deep-sea corals  $\epsilon\text{Nd}$  is a significant change of the Nd isotopic composition of the water masses that mix at the water depth of the MSW. This would imply active boundary exchange [Lacan and Jeandel, 2005a] and a rapid modification of the Nd isotopic composition of sediment deposit along the

European margin. However, it is not reasonable to postulate that the Nd isotopic compositions of the European margin sediments have changed drastically over the last 1500 years because the sedimentary sources of the Bay of Biscay are characterized by similar Nd isotopic compositions [Parra *et al.*, 1998, 1999]. In addition, it has also been shown that unradiogenic eolian dust input from North Africa ( $\epsilon\text{Nd}$   $-11$  to  $-12$  [Grousset *et al.*, 1998]) has a negligible contribution to the Nd isotopic signature of the intermediate water masses along the Iberian margin [Stumpf *et al.*, 2010]. Consequently, dissolved/particulate exchanges of sediments from the continental margin or eolian dust and seawater cannot explain the seawater  $\epsilon\text{Nd}$  variations of the last 1500 years.

[33] Several studies have indicated that in the North Atlantic, the  $\epsilon\text{Nd}$  of the main water masses has remained nearly constant through time in spite of large changes in the deepwater convection patterns over glacial/interglacial periods [Foster *et al.*, 2007; van de Flierdt *et al.*, 2006]. Recently, Arsouze *et al.* [2008], using a Global Ocean Circulation Model, suggested a minor difference of at least  $+0.5$   $\epsilon\text{Nd}$  during the Last Glacial Maximum (LGM) for northern deepwater formation, induced by sea level changes and the presence of an ice sheet over Hudson Bay, preventing boundary exchange and reducing contact with the very negative  $\epsilon\text{Nd}$  values of the continental margin during the LGM [Jeandel *et al.*, 2007]. However, over the last 1500 years, such modifications of the paleo-

geography did not occur. Hence, it is plausible to assume that the  $\epsilon\text{Nd}$  values of various North Atlantic water masses must have remained nearly identical to modern values. Furthermore, the  $\epsilon\text{Nd}$  values of MOW have most likely remained constant during the last 20 000 years [Stumpf *et al.*, 2010] and beyond [Muiños *et al.*, 2008; Khélifi *et al.*, 2009].

[34] From the above consideration, the seawater  $\epsilon\text{Nd}$  record of the last 1500 years suggests that cold periods, such as the Dark Ages Period and Little Ice Age may have been marked by changes in middepth oceanic circulation with significant variations of the water mass balance along the Western European margin. Thus, the observed moderate decrease in seawater  $\epsilon\text{Nd}$  could be induced by a weakening influence of MOW at intermediate depth along the European margin during those time intervals (Figure 6).

[35] Variability in the extend of the northward penetration of MOW has also been suggested by Lozier and Stewart [2008] for Rockall Trough, which is located further North. During the last 50 years, they observed variable northward penetration of MSW due to variations in the eastward extension of the middepth subpolar gyre correlated with changes in the NAO index. During periods of positive NAO index, they shown reduced MSW penetration into Rockall Trough induced by a greater eastward extension of the middepth subpolar gyre. Conversely, during periods of negative NAO, the subpolar gyre was confined to the West Atlantic, allowing MSW to penetrate further north, past Porcupine Bank and into Rockall Trough.

[36] Variations in the  $\epsilon\text{Nd}$  values of deep-sea corals from the Bay of Biscay that are due to an apparent weaker influence of MOW may be linked to the intermittent penetration of MSW into the Rockall Trough, illustrated by Lozier and Stewart [2008]. Thus, a greater eastward extension of the middepth subpolar gyre may also affect the hydrology of the Bay of Biscay by limiting the northward inflow of the MOW during the Dark Ages and the Little Ice Age. However, past reconstructions of the dynamics of the middepth subpolar gyre need to be further documented over the last 1500 years to confirm this hypothesis. In addition, a modification in the northward penetration of MSW along the European margin is not necessarily the only explanation for the decrease in the Nd isotopic composition of fossil deep-sea corals. Indeed, the production of MOW may have varied through time

in relation to a modification of deepwater production in the Mediterranean Sea. However, such variations in the production of Mediterranean Sea deep water during the last 1500 years is unknown and requires further investigation.

## 6. Conclusion

[37] The Nd isotopic composition analyzed in this study, for two seawater profiles, off the Iberian Peninsula and in the Bay of Biscay, display  $\epsilon\text{Nd}$  values for ENACW of  $-12.0$  off the coast of Portugal and  $-11.7$  in the Bay of Biscay. At depths corresponding to MSW, between 800 and 1200 m,  $\epsilon\text{Nd}$  values increase to  $-10.9/-11.2$  which are higher than the  $\epsilon\text{Nd}$  of MOW at the exit of the strait of Gibraltar ( $-9.4$ ). This suggests a strong dilution of this water mass by approximately 60–70% along its northward circulation, essentially with surrounding ENACW. Around 2000 m depth, the  $\epsilon\text{Nd}$  values decrease to  $-13$ , suggesting an influence of LSW, originating from the Labrador Sea. At greater depth, Nd isotopic compositions indicate the presence of another water mass (LDW), with a more radiogenic  $\epsilon\text{Nd}$  value, flowing Northward from the South Atlantic.

[38] The Nd isotopic composition of deep-sea corals (*L. pertusa*, *D. dianthus* and *M. oculata*) collected along the Western European margin present values similar to seawater and confirm the capacity for deep-sea corals to be used as a tracer of past oceanic circulation, as shown by Copard *et al.* [2010] and van de Flierdt *et al.* [2010]. Furthermore, during cold periods such as the Dark Ages and the Little Ice Age, fossil deep-sea corals highlight moderate but significantly lower  $\epsilon\text{Nd}$  values compared to present seawater  $\epsilon\text{Nd}$  values at the depth of MSW. This suggests that cooling in the Northern Hemisphere results in a weakening northward penetration of warm and saline Mediterranean water along the European margin. This reduced influence of MOW in the Bay of Biscay may be due to a greater eastward extension of the middepth subpolar gyre, as suggested by Lozier and Stewart [2008] for Rockall Trough and for the past decades and/or it may also reflect a modification of MOW export in relation to a weakening of Mediterranean deepwater formation. Further investigations are needed to establish more accurately resolved temporal records to prove a link between climate and the northward propagation of MOW along the Western European margin.

## Acknowledgments

[39] We specially thank Martin Frank and an anonymous reviewer for their constructive reviews, which significantly helped to improve this work. This work was funded through the French Agence National de Recherche projet (NEWTON: ANR-Blanc06-1-139504), the French Centre National de la Recherche Scientifique (CNRS) and the Commissariat à l'Énergie Atomique (CEA). We thank IPEV (Institut Polaire Emile Victor), the members and crew of the CAROLS cruise and Ovide cruise for their excellent work recovering deep-sea corals. In addition, we are grateful to Hans Pirlt who provided deep-sea coral from Gascogne. We further thank Eline Sallé, Claude Noury, Aliénor Lavergne and Louise Bordier for their support with U series dating and clean laboratory management. This is LSCE contribution 4609.

## References

- Ait-Ameur, N. C., and C. Goyet (2006), Distribution and transport of natural and anthropogenic CO<sub>2</sub> in the Gulf of Cadiz, *Deep Sea Res., Part II*, *53*, 1329–1343, doi:10.1016/j.dsr2.2006.04.003.
- Arsouze, T., J.-C. Dutay, M. Kageyama, F. Lacan, R. Alkama, O. Marti, and C. Jeandel (2008), A modelling sensitivity study of the influence of the Atlantic meridional overturning circulation on neodymium isotopic composition at the Last Glacial Maximum, *Clim. Past*, *4*, 191–203, doi:10.5194/cp-4-191-2008.
- Burton, K. W., and D. Vance (2000), Glacial-interglacial variations in the neodymium isotope composition of seawater in the Bay of Bengal recorded by planktonic foraminifera, *Earth Planet. Sci. Lett.*, *176*, 425–441, doi:10.1016/S0012-821X(00)00011-X.
- Cheng, H., R. L. Edwards, J. Ho, C. D. Gallup, D. A. Richards, and Y. Asmeron (2000), The half-lives of uranium-234 and thorium-230, *Chem. Geol.*, *169*, 17–33, doi:10.1016/S0009-2541(99)00157-6.
- Colin, C., N. Frank, K. Copard, and E. Douville (2010), Neodymium isotopic composition of deep-sea corals from the NE Atlantic: Implications for past hydrological changes during the Holocene, *Quat. Sci. Rev.*, *29*, 2509–2517, doi:10.1016/j.quascirev.2010.05.012.
- Copard, K., C. Colin, E. Douville, A. Freiwald, G. Gudmundsson, B. de Mol, and N. Frank (2010), Nd isotopes in deep-sea corals in the North-eastern Atlantic, *Quat. Sci. Rev.*, *29*, 2499–2508, doi:10.1016/j.quascirev.2010.05.025.
- Cronin, T. M., G. S. Dwyer, T. Kamiya, S. Schwede, and D. A. Willard (2003), Medieval Warm Period, Little Ice Age and 20th century temperature variability from Chesapeake Bay, *Global Planet. Change*, *36*, 17–29, doi:10.1016/S0921-8181(02)00161-3.
- deMenocal, P., J. Joseph Ortiz, T. Guilderson, and M. Michael Sarnthein (2000), Coherent high- and low-latitude climate variability during the Holocene warm period, *Science*, *288*, 2198–2202, doi:10.1126/science.288.5474.2198.
- Forner, S. (2005), Utilisation des CFC et du CCL4 dans l'étude de la circulation profonde de l'Atlantique Nord, M.S. thesis, Univ. de Bretagne Occidentale, Brest, Fr.
- Foster, G. L., D. Vance, and J. Prytulak (2007), No change in the neodymium isotope composition of deep water exported from the North Atlantic on glacial-interglacial time scales, *Geology*, *35*, 37–41, doi:10.1130/G23204A.1.
- Frank, N., M. Paterne, L. Ayliffe, T. Van Weering, J.-P. Henriot, and D. Blamart (2004), Eastern North Atlantic deep-sea corals: Tracing upper intermediate water  $\Delta^{14}\text{C}$  during the Holocene, *Earth Planet. Sci. Lett.*, *219*, 297–309, doi:10.1016/S0012-821X(03)00721-0.
- Grousset, F. E., M. Parra, A. Bory, P. Martinez, P. Bertrand, G. Shimmield, and R. M. Ellam, (1998), Saharan wind regimes traced by the Sr-Nd isotopic compositions of the subtropical Atlantic sediments: Last Glacial Maximum vs today, *Quat. Sci. Rev.*, *17*, 395–409, doi:10.1016/S0277-3791(97)00048-6.
- Jacobsen, S. B., and G. J. Wasserburg (1980), Sm-Nd isotopic evolution of chondrites, *Earth Planet. Sci. Lett.*, *50*, 139–155, doi:10.1016/0012-821X(80)90125-9.
- Jeandel, C. (1993), Concentration and isotopic composition of Nd in the South Atlantic Ocean, *Earth Planet. Sci. Lett.*, *117*, 581–591, doi:10.1016/0012-821X(93)90104-H.
- Jeandel, C., T. Arsouze, F. Lacan, P. Techine, and J.-C. Dutay (2007), Isotopic Nd compositions and concentrations of the lithogenic inputs into the ocean: A compilation, with an emphasis on the margins, *Chem. Geol.*, *239*, 156–164, doi:10.1016/j.chemgeo.2006.11.013.
- Keigwin, L. D., and R. S. Pickart (1999), Slope water current over the Laurentian Fan on interannual to millennial time scales, *Science*, *286*, 520–523, doi:10.1126/science.286.5439.520.
- Khélifi, N., M. Sarnthein, N. Andersen, T. Blanz, M. Frank, D. Garbe-Schönberg, B. A. Haley, R. Stumpf, and M. Weinelt (2009), A major and long-term Pliocene intensification of the Mediterranean Outflow, 3.5–3.3 Ma ago, *Geology*, *37*, 811–814, doi:10.1130/G30058A.1.
- Kuijpers, A., B. A. Malmgren, and M. S. Seidenkrantz (2009), Termination of the Medieval Warm Period: Linking sub-polar and tropical North Atlantic circulation changes to ENSO, *PAGES News*, *17*, 76–77.
- Lacan, F., and C. Jeandel (2001), Tracing Papua New Guinea imprint on the central Equatorial Pacific Ocean using neodymium isotopic compositions and Rare Earth Element patterns, *Earth Planet. Sci. Lett.*, *186*, 497–512, doi:10.1016/S0012-821X(01)00263-1.
- Lacan, F., and C. Jeandel (2004a), Denmark Strait water circulation traced by heterogeneity in neodymium isotopic compositions, *Deep Sea Res., Part I*, *51*, 71–82, doi:10.1016/j.dsr.2003.09.006.
- Lacan, F., and C. Jeandel (2004b), Subpolar Mode Water formation traced by neodymium isotopic composition, *Geophys. Res. Lett.*, *31*, L14306, doi:10.1029/2004GL019747.
- Lacan, F., and C. Jeandel (2005a), Neodymium isotopes as a new tool for quantifying exchange fluxes at the continent-ocean interface, *Earth Planet. Sci. Lett.*, *232*, 245–257, doi:10.1016/j.epsl.2005.01.004.
- Lacan, F., and C. Jeandel (2005b), Acquisition of the neodymium isotopic composition of the North Atlantic Deep Water, *Geochem. Geophys. Geosyst.*, *6*, Q12008, doi:10.1029/2005GC000956.
- Louarn, E. (2008), Étude de la variabilité de la circulation des masses d'eau profondes en Atlantique Nord en relation avec le climat: Utilisation des traceurs transitoires halocarbones, M.S. thesis, 209 pp., Univ. de Bretagne Occidentale, Brest, Fr.
- Lozier, M. S., and N. M. Stewart (2008), On the temporally varying northward penetration of Mediterranean Overflow Water and eastward penetration of Labrador Sea Water, *J. Phys. Oceanogr.*, *38*, 2097–2103, doi:10.1175/2008JPO3908.1.
- Mann, M. E., Z. Zhang, S. Rutherford, R. S. Bradley, M. K. Hughes, D. Shindell, C. Ammann, G. Faluvegi, and F. Ni

- (2009), Global signatures and dynamical origins of the Little Ice Age and Medieval Climate Anomaly, *Science*, *326*, 1256–1260, doi:10.1126/science.1177303.
- Mikkelsen, N., and A. Kuijpers (2001), *Natural Climate Variations in a Geological Perspective*, Gads Forlag, Copenhagen.
- Muñios, S. B., M. Frank, C. Maden, J. R. Hein, T. van de Flierdt, S. M. Lebreiro, L. Gaspar, J. H. Monteiro, and A. N. Halliday (2008), New constraints on the Pb and Nd isotopic evolution of NE Atlantic water masses, *Geochem. Geophys. Geosyst.*, *9*, Q02007, doi:10.1029/2007GC001766.
- Parra, M., H. Trouky, J. M. Jouanneau, F. Grousset, C. Latouche, and P. Castaing (1998), Etude isotopique (Sr-Nd) de l'origine des dépôts fins holocènes du littoral atlantique (S-O France), *Oceanol. Acta*, *21*, 631–644, doi:10.1016/S0399-1784(99)80022-X.
- Parra, M., P. Castaing, J. M. Jouanneau, F. Grousset, and C. Latouche (1999), Nd-Sr isotopic composition of present-day sediments from the Gironde estuary, its draining basins and the WestGironde mud patch (SW France), *Cont. Shelf Res.*, *19*, 135–150.
- Piepgas, D. J., and G. J. Wasserburg (1983), Influence of the Mediterranean outflow on the isotopic composition of Neodymium in waters of the North Atlantic, *J. Geophys. Res.*, *88*, 5997–6006, doi:10.1029/JC088iC10p05997.
- Piepgas, D. J., and G. J. Wasserburg (1987), Rare Earth element transport in the western North Atlantic inferred from Nd isotopic observations, *Geochim. Cosmochim. Acta*, *51*, 1257–1271, doi:10.1016/0016-7037(87)90217-1.
- Piotrowski, A. M., S. L. Goldstein, S. R. Hemming, and R. G. Fairbanks (2004), Intensification and variability of ocean thermohaline circulation through the last deglaciation, *Earth Planet. Sci. Lett.*, *225*, 205–220, doi:10.1016/j.epsl.2004.06.002.
- Piotrowski, A. M., S. L. Goldstein, S. R. Hemming, and R. G. Fairbanks (2005), Temporal Relationships of carbon cycling and ocean circulation at glacial boundaries, *Science*, *307*, 1933–1938, doi:10.1126/science.1104883.
- Rhein, M., and H. H. Hinrichsen (1993), Modification of Mediterranean Water in the Gulf of Cadiz, studied with hydrographic, nutrient and chlorofluoromethane data, *Deep Sea Res., Part I*, *40*, 267–291, doi:10.1016/0967-0637(93)90004-M.
- Rickli, J., M. Frank, and A. N. Halliday (2009), The hafnium-neodymium isotopic composition of Atlantic seawater, *Earth Planet. Sci. Lett.*, *280*, 118–127, doi:10.1016/j.epsl.2009.01.026.
- Spivack, A. J., and G. J. Wasserburg (1988), Neodymium isotopic composition of the Mediterranean outflow and the eastern North Atlantic, *Geochim. Cosmochim. Acta*, *52*, 2767–2773, doi:10.1016/0016-7037(88)90144-5.
- Stumpf, R., M. Frank, J. Schönfeld, and B. A. Haley (2010), Late Quaternary variability of Mediterranean Outflow Water from radiogenic Nd and Pb isotopes, *Quat. Sci. Rev.*, *29*, 2462–2472, doi:10.1016/j.quascirev.2010.06.021.
- Tachikawa, K., V. Athias, and C. Jeandel (2003), Neodymium budget in the modern ocean and paleo-oceanographic implications, *J. Geophys. Res.*, *108*(C8), 3254, doi:10.1029/1999JC000285.
- Tachikawa, K., M. Roy-Barman, A. Michard, D. Thouron, D. Yeghicheyan, and C. Jeandel (2004), Neodymium isotopes in the Mediterranean Sea: Comparison between seawater and sediment signals, *Geochim. Cosmochim. Acta*, *68*, 3095–3106, doi:10.1016/j.gca.2004.01.024.
- van Aken, H. M. (2000), The hydrography of the mid-latitude northeast Atlantic Ocean: I: The deep water masses, *Deep Sea Res., Part I*, *47*, 757–788, doi:10.1016/S0967-0637(99)00092-8.
- Vance, D., and K. Burton (1999), Neodymium isotopes in planktonic foraminifera: A record of the response of continental weathering and ocean circulation rates to climate change, *Earth Planet. Sci. Lett.*, *173*, 365–379, doi:10.1016/S0012-821X(99)00244-7.
- van de Flierdt, T., L. F. Robinson, J. F. Adkins, S. R. Hemming, and S. L. Goldstein (2006), Temporal stability of the neodymium isotope signature of the Holocene to glacial North Atlantic, *Paleoceanography*, *21*, PA4102, doi:10.1029/2006PA001294.
- van de Flierdt, T., L. F. Robinson, and J. F. Adkins (2010), Deep-sea corals aragonite as a recorder for the neodymium isotopic composition of seawater, *Geochim. Cosmochim. Acta*, *74*, 6014–6032, doi:10.1016/j.gca.2010.08.001.
- Vogler, S., J. Scholten, M. Rutgers van der Loeff, and A. Mangini (1998), <sup>230</sup>Th in the eastern North Atlantic: The importance of water mass ventilation in the balance of <sup>230</sup>Th, *Earth Planet. Sci. Lett.*, *156*, 61–74, doi:10.1016/S0012-821X(98)00011-9.